Approach to Cystic Lesions in the Abdomen and Pelvis, with Radiologic-Pathologic Correlation

Joseph H. Yacoub, MD
Jennifer A. Clark, MD
Edina E. Paal, MD
Maria A. Manning, MD

Abbreviations: CSF = cerebrospinal fluid, EDC = enteric duplication cyst, H-E = hematoxylin-eosin, MCN = mucinous cystic neoplasm, MCPM = multicystic peritoneal mesothelioma, PMP = pseudomyxoma peritonei

RadioGraphics 2021; 41:1368–1386

https://doi.org/10.1148/rg.2021200207

Content Codes: CT GI GU MR

From the Department of Radiology, MedStar Georgetown University Hospital, 3800 Reservoir Rd NW, Washington, DC 20007 (J.H.Y., J.A.C., M.A.M.); Pathology and Laboratory Medicine Service, VA Medical Center, Washington, DC (E.E.P.); Department of Pathology, George Washington University School of Medicine and Health Sciences, Washington, DC (E.E.P.); and American Institute for Radiologic Pathology, Silver Spring, Md (M.A.M.). Received January 14, 2021; revision requested March 5 and received June 14; accepted June 15. For this journal-based SA-CME activity, the author M.A.M. has provided disclosures (see end of article); all other authors, the editor, and the reviewers have disclosed no relevant relationships. **Address correspondence to** M.A.M. (e-mail: *mmanning@acr.org*).

SA-CME LEARNING OBJECTIVES

After completing this journal-based SA-CME activity, participants will be able to:

- Recognize the different types of cystic lesions in the abdomen or pelvis categorized on the basis of their causes and classification.
- Describe the key pathologic and imaging features of cystic-appearing lesions in the abdomen or pelvis, including locularity, wall thickness, and presence of internal septa, mural nodularity, or calcifications.
- Formulate a differential diagnosis for a cystic-appearing lesion in the abdomen or pelvis, considering its location or site of origin and imaging features.

See rsna.org/learning-center-rg.

Cystic lesions found in and around the peritoneal cavity can often be challenging to diagnose owing to significant overlap in imaging appearance between the different entities. When the cystic lesion can be recognized to arise from one of the solid abdominal organs, the differential considerations can be more straightforward; however, many cystic lesions, particularly when large, cannot be clearly associated with one of the solid organs. Cystic lesions arising from the mesentery and peritoneum are less commonly encountered and can be caused by relatively rare entities or by a variant appearance of less-rare entities. The authors provide an overview of the classification of cystic and cystic-appearing lesions and the basic imaging principles in evaluating them, followed by a summary of the clinical, radiologic, and pathologic features of various cystic and cystic-appearing lesions found in and around the peritoneal cavity, organized by site of origin. Emphasis is given to lesions arising from the mesentery, peritoneum, or gastrointestinal tract. Cystic lesions arising from the liver, spleen, gallbladder, pancreas, urachus, adnexa, or soft tissue are briefly discussed and illustrated with cases to demonstrate the overlap in imaging appearance with mesenteric and peritoneal cystic lesions. When approaching a cystic lesion, the key imaging features to assess include cyst content, locularity, wall thickness, and presence of internal septa, solid components, calcifications, or any associated enhancement. While definitive diagnosis is not always possible with imaging, careful assessment of the imaging appearance, location, and relationship to adjacent structures can help narrow the differential diagnosis.

Online supplemental material is available for this article.

Introduction

Cystic-appearing lesions are commonly encountered in and around the peritoneal cavity. Differentiating between types of cystic lesions using imaging is challenging owing to their significant appearance overlap. When the organ of origin is obvious, the radiologist can focus on the organ-based differential diagnosis for a cystic mass. However, many cystic lesions, particularly when large, cannot be clearly associated with any one organ. Moreover, lesions arising from the peritoneal surface, omentum, mesentery, adnexa, or gastrointestinal tract develop within the same general anatomic space. Differentiation is further complicated by controversy and confusion around the classification of cystic lesions that arise in and around the mesentery (1).

Cystic lesions arising from or within the peritoneum, mesentery, or gastrointestinal tract may be broadly grouped into true cysts, cystic neoplasms, and cystic-appearing lesions—including inflammatory, infectious, and iatrogenic lesions—and careful assessment of cyst content and structural features can help narrow the differential diagnosis. True cysts (mesenteric cysts) are typically benign-appearing lesions

TEACHING POINTS

- True cysts are lined by epithelium, endothelium, or mesothelium, depending on the tissue of origin; pseudocysts lack such a lining. Collections of necrotic tissue, pus, hemorrhage, or loculated ascites can be indistinguishable from true cysts at imaging.
- In describing the cystic lesion, any deviation from the simple appearance should be described. Atypical appearances include multilocularity, wall thickening, internal septa and enhancement, solid internal components, and the presence of calcifications.
- Mesenteric cysts are uncommon lesions with variable pathogenesis and confusing terminology. The term *mesenteric cyst* is simply descriptive of the location and gross appearance of any cyst arising in the mesentery.
- MCPM is known by various names in the literature, including peritoneal inclusion cyst, multilocular inclusion cyst, multicystic mesothelioma, and benign multicystic mesothelioma, reflecting the uncertainties around lesion pathogenesis.
- Cystic-appearing lesions in the abdomen and pelvis can have a broad differential diagnosis encompassing neoplastic, inflammatory, congenital, and iatrogenic lesions. While some lesions are truly cystic, others may represent necrosis, cystic degeneration, hematomas, or reactive collections. The distinction may not always be evident at imaging; however, careful assessment of the imaging appearance, location, relationship to surrounding structures, and clinical context may help narrow the differential diagnosis and guide management.

with thin walls, no solid nodules, and only rare calcifications. Differentiating features include cyst content (simple serous, although a fat-fluid level can be seen in chylolymphatic cyst) and locularity (unilocular except for cystic lymphangiomas, which are characteristically multilocular).

Cystic neoplasms (mucinous cystic neoplasm [MCN], multicystic peritoneal mesothelioma [MCPM], pseudomyxoma peritonei [PMP]) are more complex, with multilocularity, septa, and calcifications. Solid nodules are rare, and when present, are worrisome. Thickened calcified walls are most commonly associated with inflammatory, infectious, and iatrogenic cystic lesions. Finally, soft-tissue neoplasms or lymph nodes with central necrosis or cystic change can mimic a cystic lesion and should be considered for thick-walled complex cystic lesions with large solid components.

In this article, we review the clinical, radiologic, and pathologic features of cysts and cystic-appearing lesions occurring in and around the peritoneal cavity to provide a framework for establishing a differential diagnosis when a cystic lesion is next encountered.

Classification of Cystic Lesions in Abdomen

Cystic-appearing lesions arising in the peritoneal cavity can be classified according to their cause (congenital, neoplastic, reactive or proliferative, infectious or inflammatory, iatrogenic or traumatic) (1) or histologic definition (true cysts, pseudocysts, trapped fluid, solid lesions mimicking a cyst) (Table 1). True cysts are lined by epithelium, endothelium, or mesothelium, depending on the tissue of origin; pseudocysts lack such a lining. Collections of necrotic tissue, pus, hemorrhage, or loculated ascites can be indistinguishable from true cysts at imaging.

Basic Imaging Principles of Cystic Lesions

At US, simple cysts are well-defined, anechoic, spheroid structures with posterior acoustic enhancement and no internal flow at color Doppler imaging. The presence of hemorrhage or debris within a cystic lesion will introduce internal echoes, which may complicate distinction from solid lesions. US is an excellent, cost-effective, and readily accessible modality for evaluating suspected cysts, but with increasing cyst complexity or size, CT or MRI may be needed for further evaluation.

At CT, a cyst appears as a well-defined spheroid lesion with homogeneous near-water attenuation (0–20 HU). Cyst contents can be divided into three categories: homogeneous near-water attenuation, suggesting simple fluid; lower-than-water attenuation and fluid-fluid levels, suggesting chylous fluid and lipid contents; and higher-than-water attenuation, which can be homogeneous or heterogeneous owing to the presence of proteinaceous material, hemorrhage, or necrotic tissue.

At MRI, simple cystic lesions have marked T2-weighted hyperintensity and low T1-weighted signal intensity. Known simple fluid, such as cerebrospinal fluid (CSF), can be used as a reference. The presence of proteinaceous or hemorrhagic products in the cyst decreases T2-weighted hyperintensity and increases T1-weighted signal intensity. This increased T1-weighted signal intensity can make visual assessment of enhancement difficult, and subtraction postprocessing (subtracting precontrast images from postcontrast images) can aid in detecting subtle low-grade enhancement, a notable advantage of MRI. The presence of pus or hemorrhage can restrict diffusion at diffusion-weighted imaging (DWI), thus mimicking neoplasm, mandating detection of even subtle enhancement. Lipid signal intensity within fat or chylous fluid is confirmed with fat-suppression or chemical shift artifact sequences.

In describing the cystic lesion, any deviation from the simple appearance should be described. Atypical appearances include multilocularity,

Table 1: Classification of Cystic Lesions Arising in the Abdomen by Cause and Histologic Definition

Entity by Cause	Pathologic Definition
Congenital	
Chylolymphatic mesenteric cyst	Cyst with endothelial lining
Cystic lymphangioma	
Enteric duplication cyst (EDC)	Cyst with epithelial lining
Enteric cyst	
Mature cystic teratoma	
Urachal cyst	
Peritoneal simple mesothelial cyst (PSMC)	Cyst with mesothelial lining
Neoplastic	
Mucinous cystic neoplasm (MCN)	Cyst with epithelial lining
Gastrointestinal stromal tumor (GIST)	Tumor with necrotic or cystic degeneration
Soft-tissue sarcoma	
Desmoid tumor	
Reactive or proliferative	
Multicystic peritoneal mesothelioma (MCPM)	Cyst with mesothelial lining
Infectious or inflammatory	
Abscess	Pseudocyst or trapped fluid
Nonpancreatic pseudocyst	
Peritoneal hydatidosis	
Peritoneal tuberculosis	
Iatrogenic or traumatic	
Nonpancreatic pseudocyst	Pseudocyst
Cerebrospinal fluid (CSF) pseudocyst	
Lymphocele	
Gossypiboma	

wall thickening, internal septa and enhancement, solid internal components, and the presence of calcifications.

Cystic Lesions of Mesentery and Peritoneum

Benign True Cysts of Mesentery and Peritoneum

Mesenteric Cysts.—Mesenteric cysts are uncommon lesions with variable pathogenesis and confusing terminology. The term *mesenteric cyst* is simply descriptive of the location and gross appearance of any cyst arising in the mesentery. Histologically, many entities are included under this umbrella terminology, including mesothelium-lined peritoneal simple mesothelial cyst (PSMC); endothelium-lined chylolymphatic mesenteric cyst or cystic lymphangioma; epithelium-lined enteric duplication cyst (EDC) or enteric cyst; and fluid collections with no cellular lining, such as nonpancreatic pseudocysts.

Peritoneal Simple Mesothelial Cyst.—PSMC is a congenital cyst formed in the small bowel, mesentery, mesocolon, or omentum (2), presumably after failure of the mesothelium-lined peritoneal surfaces to coalesce. Mesothelium-lined cysts have also been reported to arise from the pericardium (3) and round ligament of the liver (4). PSMC is typically reported in children and young adults (2) but has been reported in older adults (Fig 1) (5). Usually asymptomatic, it can manifest with nonspecific abdominal symptoms including pain, distention, bloating, constipation, and vomiting (2,5). Children can present with acute abdomen due to rupture, inflammation, infection, torsion, or hemorrhage within the cyst (2).

Pathologic examination reveals a thin-walled unilocular cyst (Fig 1), usually containing serous fluid, of varying size (range, 2–40 cm) (2). Flat or cuboidal mesothelial cells line the inner surface, and the cyst wall is fibrotic (Fig 1) (2). The mesothelial cells lining the cyst can be further characterized with immunohistochemistry and stain positive for cytokeratin 5/6, cytokeratin 7 (CK7), calretinin, and WT1 protein and negative for vascular markers such as CD31 (4).

CT, MRI, or US reveals a simple-appearing thin-walled unilocular cyst without internal septa (Fig 1) (6).

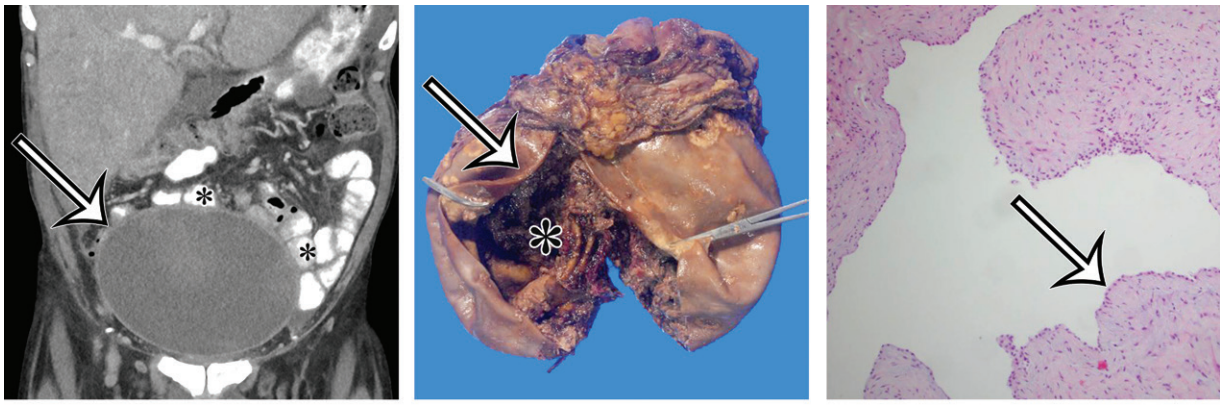

a. b. c.

Figure 1. PSMC incidentally identified in a 68-year-old man, with pathologic correlation. **(a)** Coronal contrast-enhanced CT image shows a unilocular thin-walled cyst (arrow) in the midline pelvis, intimately associated with multiple small-bowel loops (*). There are no septa or solid components. **(b)** Photograph of the cut resected specimen shows the smooth thin tan cyst wall (arrow), with few internal blood products (*). **(c)** Low-power photomicrograph shows flattened cuboidal mesothelial cells lining the cyst with normal cytoplasm (arrow). (Hematoxylin-eosin [H-E] stain; original magnification, ×4.)

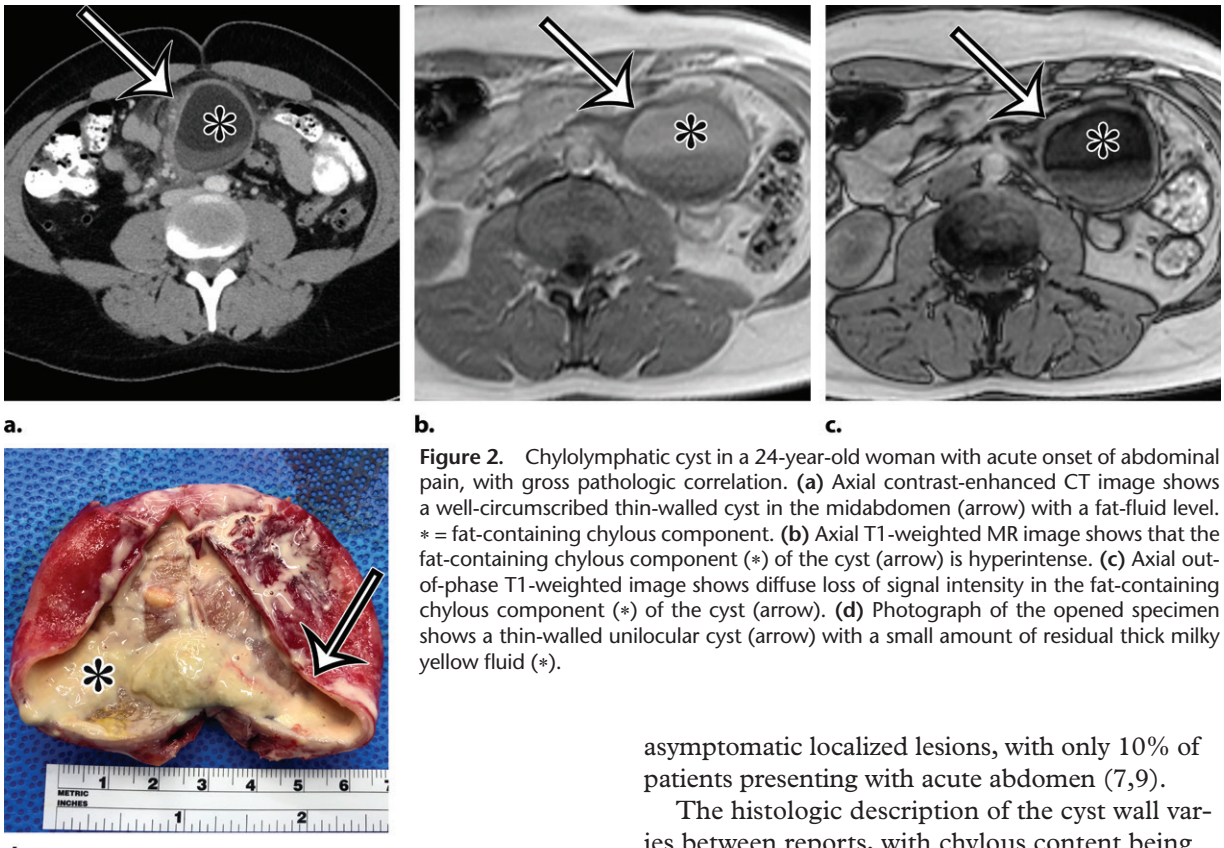

a. b. c. d.

Figure 2. Chylolymphatic cyst in a 24-year-old woman with acute onset of abdominal pain, with gross pathologic correlation. **(a)** Axial contrast-enhanced CT image shows a well-circumscribed thin-walled cyst in the midabdomen (arrow) with a fat-fluid level. * = fat-containing chylous component. **(b)** Axial T1-weighted MR image shows that the fat-containing chylous component (*) of the cyst (arrow) is hyperintense. **(c)** Axial out-of-phase T1-weighted image shows diffuse loss of signal intensity in the fat-containing chylous component (*) of the cyst (arrow). **(d)** Photograph of the opened specimen shows a thin-walled unilocular cyst (arrow) with a small amount of residual thick milky yellow fluid (*).

Chylolymphatic Mesenteric Cyst.—Chylolymphatic mesenteric cyst contains chylous fluid and originates from the small-bowel mesentery (7). The true nature and cause of this cyst are unclear; some authors consider it a type of cystic lymphangioma, while others describe it as a variant of mesenteric cysts (8). It is mainly seen in adults, with a slight female predominance. In contrast to cystic lymphangioma, there are few reports in the pediatric population, and these tend to manifest as asymptomatic localized lesions, with only 10% of patients presenting with acute abdomen (7,9).

The histologic description of the cyst wall varies between reports, with chylous content being the most common defining feature (Fig 2). Some authors describe a striking resemblance between chylolymphatic mesenteric cyst and cystic lymphangioma, both grossly and microscopically (8,9); however, chylolymphatic cysts lack the disorganized smooth muscle layer seen in cystic lymphangioma (9).

At imaging, they appear as unilocular cysts with a fluid-fluid level composed of nondependent chyle (Fig 2). When assessing with real-time US, the contents can be mixed by shaking or moving the patient, with reformation of the fluid-fluid

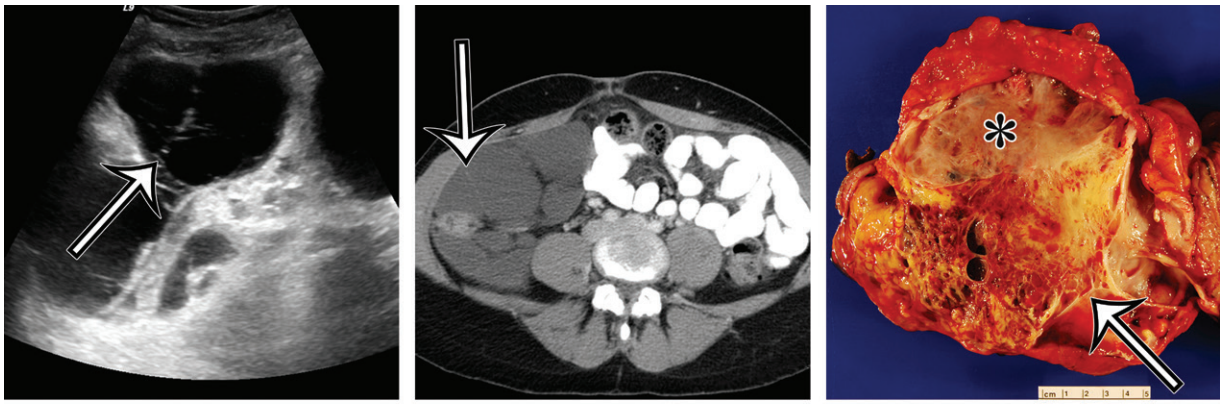

a. b. c.

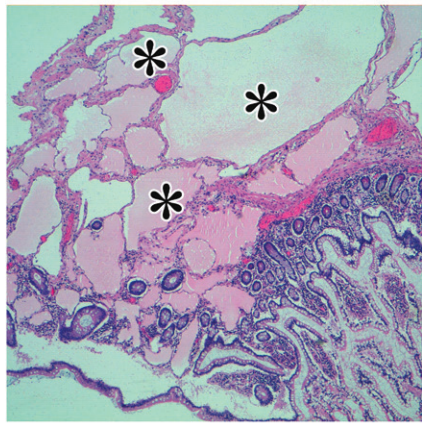

d.

Figure 3. Cystic lymphangioma in a 33-year-old woman with a 2-week history of right lower quadrant pain, with pathologic correlation. **(a, b)** Transverse US **(a)** and axial contrast-enhanced CT **(b)** images show a thin-walled multiloculated cyst containing thin septa (arrow) that insinuates around the colon. **(c)** Photograph of the cut gross specimen shows the multilocular nature of the lymphangioma, with cystic spaces of varying size (∗) and thin septa (arrow). **(d)** Photomicrograph of a cystic lymphangioma shows multiple thin-walled cystic spaces lined with endothelial cells and containing lymph (∗). (MRI features are shown in Figure E1.)

level after 30 minutes at rest (10). At MRI, the fat content of the chyle can be shown as T1 and T2 hyperintense, with loss of signal intensity on T1-weighted out-of-phase and fat-suppressed images (Fig 2).

Cystic Lymphangioma.—Cystic lymphangioma, also known as cavernous lymphangioma, mesenteric lymphangioma, or lymphangiomatosis, is a benign proliferative malformation of the lymphatic system (11). This congenital lesion develops from embryonic sequestration of lymphatic tissue and can occur throughout the body, most commonly in the neck and axilla; the majority of intraperitoneal cystic lymphangiomas occur in the small-bowel mesentery (12). Although reported most often in the pediatric population, they have been reported in adults (more often in men than in women) (12,13). Most often asymptomatic, they can manifest with subacute abdominal pain due to mass effect or bowel obstruction (12). They are seldom complicated by infection, hemorrhage, perforation, or rupture (12).

Pathologically, a lymphangioma is a thin-walled cystic mass with a yellow external surface and thin internal septa dividing the mass into multiple irregular spaces of varying size (Fig 3). The fluid contents are predominantly chylous but may be serous or hemorrhagic (Fig E1) (6,12). They consist of endothelium-lined spaces surrounded by a connective tissue stroma of varying thickness containing lymphoid tissue and occasionally smooth muscle (Fig 3) (11).

The gross pathologic appearance is nicely depicted at multimodality imaging (Fig 3). Contrast-enhanced CT shows enhancement of the wall and septa (Fig 3, Fig E1) (6,11). Calcifications are rare (11). Intrinsic attenuation can vary from near-water to fat attenuation, depending on the amount of chyle present. MRI is the most useful imaging modality to show the multiseptated cystic appearance characteristic of lymphangioma, which typically has high T2-weighted and low T1-weighted signal intensity (Fig E1). When a lymphangioma contains large amounts of chyle, the internal contents may demonstrate high T1-weighted and intermediate T2-weighted signal intensity.

The presence of superimposed hemorrhage or infection may complicate the appearance of lymphangioma with all imaging modalities. It can mimic a solid lesion at noncontrast examinations. Lymphangiomas are locally infiltrative and tend to grow slowly along tissue planes (6). Because they can be insinuated between bowel loops, they might be mistaken for ascites; however, the presence of septa, mass effect on bowel loops, and lack of fluid in dependent recesses can offer important clues to make the distinction (Fig 3) (6).

Cystic Neoplasms of Mesentery and Peritoneum

MCN of Mesentery.—Extraovarian MCN is lined by mucin-producing epithelial cells and occurs

in multiple abdominal locations, most commonly the pancreas, appendix, and hepatobiliary tract (14). MCN can arise from the mesentery of the small intestine, mesocolon, or mesoappendix; less than 20 cases have been reported in the literature as of 2012 (14,15). According to the most recent World Health Organization (WHO) classification, MCN is categorized as low grade or high grade (16). Rare cases have an associated invasive carcinoma component (14). MCN manifests almost exclusively in women (14,15) (median age, 34.2 years), with low-grade lesions occurring more frequently in slightly younger patients (median age, 31.9 years) compared with high-grade lesions (median age, 38.2 years) (15). MCN tends to manifest with vague nonspecific symptoms such as chronic diffuse abdominal pain.

Grossly, MCN manifests as a cystic mass with a thick fibrous wall. The loculi contain thick mucin or hemorrhagic necrotic material. Most have smooth internal surfaces; the rare highly dysplastic or invasive MCN often has nodules or papillary projections. Histologically, MCN is lined by mucin-secreting columnar epithelium associated with a subepithelial ovarian-type stroma.

At US, CT, or MRI, MCN typically appears as a multiloculated cystic mass. Rim and septal calcification have been described (15). The loculi can contain simple or proteinaceous fluid. As with other mucinous cystic neoplasms, solid or nodular components are rare, but when present should raise concern for invasiveness (15).

Definitive diagnosis with imaging is challenging owing to rarity and overlap with other cystic lesions. Most important in imaging evaluation is delineation of the site of origin; however, this can be increasingly difficult with increasing tumor size. Of note, aspiration of the cyst content is unlikely to yield a definitive diagnosis.

Multicystic Peritoneal Mesothelioma.—MCPM is known by various names in the literature, including peritoneal inclusion cyst, multilocular inclusion cyst, multicystic mesothelioma, and benign multicystic mesothelioma, reflecting the uncertainties around lesion pathogenesis. The prevailing theory of a chronic irritant causing nonneoplastic reactive mesothelial proliferation and cyst formation (17) is supported by the fact that MCPM occurs predominantly in premenopausal patients who have functioning ovaries and pelvic adhesions with impaired absorption of peritoneal fluid secondary to pelvic surgery, pelvic trauma, endometriosis, or pelvic inflammatory disease (6). Some authors believe that endometriosis contributes to the origin of MCPM, supported by the presence of small foci of endometriosis in the wall of the cysts (17). Alternatively, because it can recur locally and rarely undergoes malignant transformation, some believe this to be a mesothelial neoplasm (18).

Most patients are asymptomatic until the lesion grows large enough to become bothersome; symptoms include chronic intermittent abdominal pain, tenderness, palpable mass, weight loss, dyspareunia, constipation, and urinary hesitancy or frequency (6,17). Rarely, MCPM has been described in men, accounting for up to 16% of cases (18), typically arising from the peritoneal surface along the superior bladder wall or in the retrovesical space (6). MCPM occurs most often in the pelvic peritoneum, in the cul-de-sac, or along the peritoneal surfaces of the uterus and rectum (Fig 4) (17,18). Multifocality, freely floating cysts, and unilocular cysts have been reported (18).

MCPM tends to be large, approximating 13 cm in diameter (17). It grossly appears as thin-walled translucent cysts arranged in a grapelike form (Fig 4). They are mostly composed of serous fluid, with occasional mucinous, gelatinous, or hemorrhagic contents. Definitive diagnosis requires histologic evaluation, at which it appears as multiple cystic spaces lined by a single layer of flattened or cuboidal mesothelial cells surrounded by a delicate thin fibrovascular stroma (Fig 4). Immunohistochemistry allows confirmation of the diagnosis by demonstrating positivity for mesothelial markers, including cytokeratin 5/6, calretinin, and transcription factor WT1 and negativity for endothelial markers CD31, CD34, and factor VIII (Fig 4) (17). A high serum concentration of cancer antigen 19-9 (CA 19-9) has been associated with a diagnosis of MCPM (17).

At imaging, MCPM appears as multiloculated thin-walled cystic lesions, frequently adhered to the adnexa (Fig 4). Entrapment of the ovaries within the multiloculated lesion, the so-called spider-in-web appearance, is a characteristic finding (17). The cystic fluid may contain echoes from debris or hemorrhage; nodular excrescences or thick, polypoid, and incomplete septa may be present (6). Vessels in the mesothelium-lined septa can result in low-resistance flow.

CT demonstrates the full magnitude of the lesions, which can extend to the upper abdomen. Calcification has not been described (18). MRI is considered the best imaging technique for demonstrating the anatomic relation of the mass with the pelvic structures (6,17). At MRI, the cysts have high T2-weighted and low T1-weighted signal intensity, unless hemorrhage is present, which could result in higher signal intensity on precontrast T1-weighted images (Fig 4). The septa commonly enhance (18).

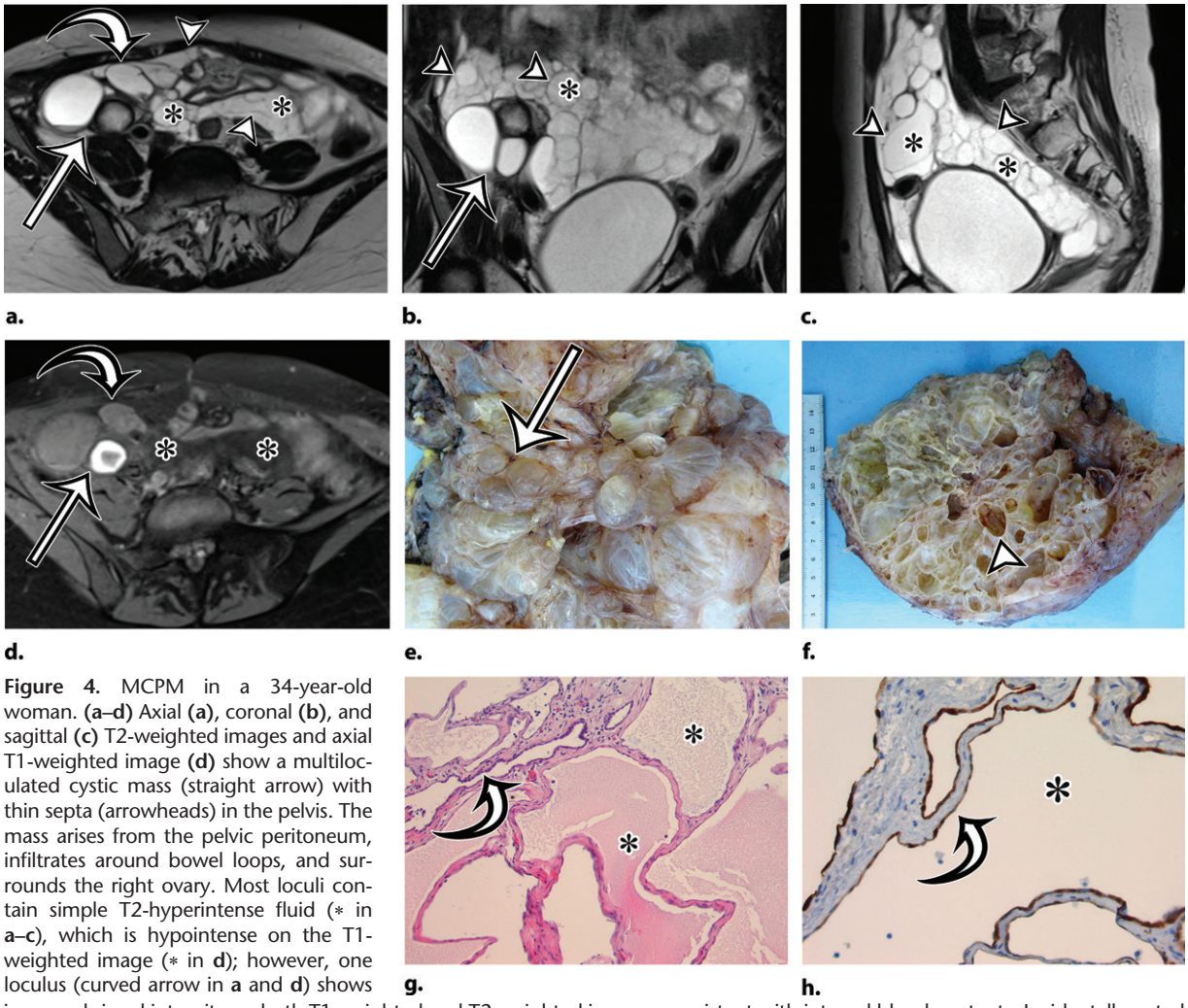

Figure 4. MCPM in a 34-year-old woman. **(a–d)** Axial **(a)**, coronal **(b)**, and sagittal **(c)** T2-weighted images and axial T1-weighted image **(d)** show a multiloculated cystic mass (straight arrow) with thin septa (arrowheads) in the pelvis. The mass arises from the pelvic peritoneum, infiltrates around bowel loops, and surrounds the right ovary. Most loculi contain simple T2-hyperintense fluid (∗ in **a–c**), which is hypointense on the T1-weighted image (∗ in **d**); however, one loculus (curved arrow in **a** and **d**) shows increased signal intensity on both T1-weighted and T2-weighted images, consistent with internal blood contents. Incidentally noted are T1-hyperintense hemorrhagic cysts in the right ovary (straight arrow in **d**); the lateral cyst contains layering T1-hyperintense blood products, and the superomedial cyst has a T2-hypointense rim (straight arrow in **a**). **(e, f)** Photographs of a whole **(e)** and cut **(f)** gross specimen show the multicystic nature of a peritoneal mesothelioma, with a grapelike appearance of the whole specimen (arrow in **e**). The cut specimen shows the mass to be comprised of innumerable cystic spaces of varying size separated by a thin fibrovascular stroma (arrowhead in **f**), which matches the appearance at MRI. **(g, h)** High-power photomicrographs with H-E stain **(g)** and calretinin immunohistochemical stain **(h)** show multiple small cystic spaces (∗) lined by cuboidal mesothelium (arrow), which stains positive for calretinin, a mesothelial marker. (Original magnification, ×100.)

Pseudomyxoma Peritonei.—PMP is not a pathologic entity but rather a clinical or radiologic term describing the finding of copious thick mucinous or gelatinous material on the peritoneal surfaces of the abdomen (19). The reported incidence is one to two cases per million per year (19,20), with women more susceptible than men, at a mean age of 53 years (20). Patients present with progressive abdominal pain, increasing abdominal girth, and weight loss.

The peritoneal deposits are comprised of benign mucin and mucinous epithelial cells (ranging from benign epithelium to adenocarcinoma). Pathologic classification is contentious, with a recent consensus article classifying PMP by the presence and histologic features of epithelial cells (mucin only, low-grade dysplasia, high-grade dysplasia, presence of signet ring cells) and including deposits associated with mucinous carcinomas of the appendix, gastrointestinal tract, gallbladder, pancreas, or ovary (21). Some pathologists limit the term *pseudomyxoma peritonei* to only acellular mucin and low-grade mucinous carcinoma peritonei originating from low-grade appendiceal mucinous neoplasms (LAMNs), also known as disseminated peritoneal adenomucinosis (DPAM) (19,22). Low-grade PMP or DPAM has a better prognosis than high-grade PMP associated with mucinous adenocarcinomas arising from other organs, also referred to as peritoneal mucinous carcinomatosis (PMCA).

At imaging, PMP is characterized as thick mucinous material found throughout the peritoneal cavity. When copious, it can exert mass effect

a. b. c.

Figure 5. PMP in a 57-year-old man. **(a)** Sagittal US image shows masslike expansion of the omentum with echogenic septa (arrow) surrounded by hypoechoic gelatinous fluid. The subjacent bowel loops are displaced centrally. **(b)** Axial contrast-enhanced CT image shows low-attenuation fluid surrounding the liver and displacing the stomach, with scalloping of the hepatic surface (arrow), which represents extrinsic pressure from the mucinous implants. **(c)** Coronal T2-weighted image shows scalloping of the intraperitoneal visceral surfaces (straight arrow) and heterogeneous signal intensity of the fluid (curved arrow), which allow differentiation of PMP from simple ascites.

on the solid organs, with a scalloping appearance along the surfaces; most commonly involving the liver and spleen surfaces, this allows differentiation of PMP from simple ascites (Figs 5, 6). At US, the mucin may appear hyperechoic owing to gelatinous contents (19). Hyperechoic septa are often present, representing the edges of the mucinous nodules. Omental and parietal peritoneal implants manifest as focal or sheetlike echogenic masses (Fig 5).

At CT, mucin is hypoattenuating. Soft-tissue-attenuation septa and solid components—comprised of compressed mesentery, fibrosis and solid tumor, and calcifications—may be present. CT is helpful in assessing tumor burden; mucin tends to follow the route of normal peritoneal flow, with early mucinous deposits accumulating in the pouch of Douglas in women or the retrovesical space in men, then spreading to the right lower quadrant near the ileocecal junction, right subhepatic space, and right subphrenic space (19). As PMP progresses, it tends to spare the peritoneal surfaces of the bowel and to accumulate beneath the right hemidiaphragm; along the omental surfaces; and in the gravity-dependent portions of the pelvis, right retrohepatic space, right subhepatic space, and left paracolic gutter (19). In the late stages, involvement of the root of the mesentery and small-bowel serosa may lead to obstruction.

MRI has not been extensively studied in PMP; existing reports demonstrate similar findings to those of CT. The mucin is more heterogeneous than simple fluid, allowing distinction from simple ascites (Figs 5, 6), and enhancement of the tumor components may be better delineated with subtraction imaging. When these findings are present, it is important to carefully assess the appendix for a primary tumor.

Differentiating low-grade PMP (DPAM) from peritoneal mucinous carcinomatosis (PMCA) at imaging is difficult owing to overlapping features, despite a vastly different clinicopathologic course. Features that favor mucinous carcinomatosis include invasion of visceral organs, involvement of the intestinal serosal surface, pleural effusions and masses, and spread by lymphatic or hematogenous routes (19). Features favoring acellular mucin and low-grade PMP (DPAM) include extensive scalloping of the liver and spleen, loculation of the intraperitoneal mucin, curvilinear calcifications, and presence of mucin or a soft-tissue mass on the appendix (22).

Infectious and Inflammatory Cysts of Mesentery and Peritoneum

Nonpancreatic Pseudocyst.—Nonpancreatic pseudocysts are lesions arising from the mesentery or omentum secondary to trauma, surgery, or infection. They are sequelae of liquefaction in a hematoma or abscess that failed to reabsorb completely encased in a thick fibrous wall (6). Subsets of nonpancreatic intraperitoneal pseudocysts include CSF pseudocyst and lymphocele.

CSF pseudocyst is a relatively uncommon complication of a ventriculoperitoneal (VP) shunt (23), thought to reflect fluid buildup after inflammatory reaction around the catheter tip related to clinical or subclinical shunt infection after abdominal operation or shunt revision. It is reported to develop between 2 weeks and 21 years after VP shunt placement (24). CSF pseudocyst can form anywhere in the abdominal cavity, most rarely in the liver in a subcapsular or intraparenchymal location (Fig 7) (25–30). It can also occur in the abdominal wall (31). Lymphocele is a loculated collection formed after

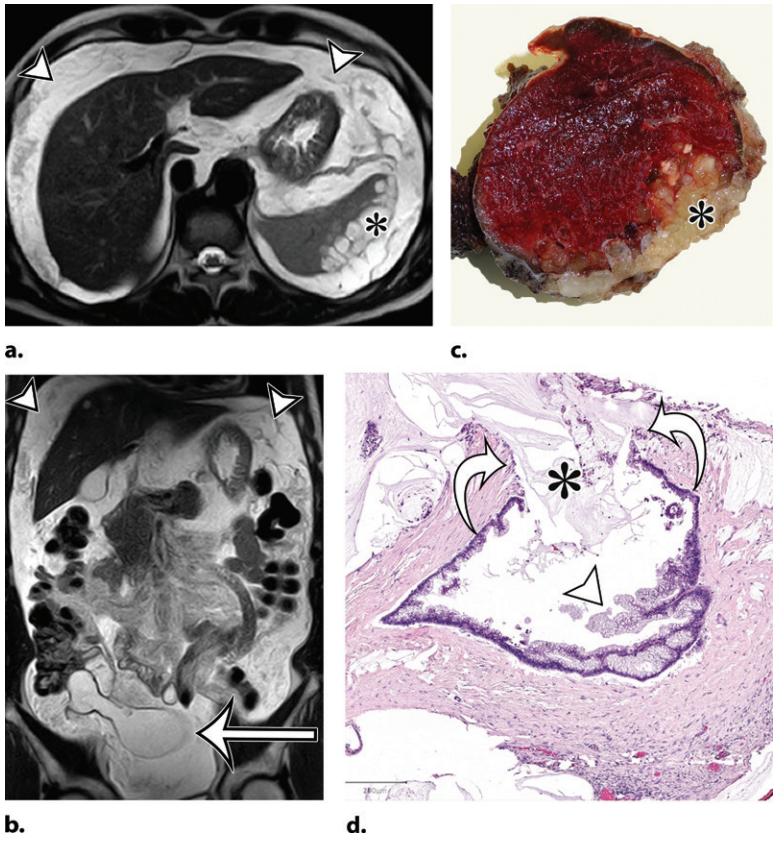

Figure 6. PMP (disseminated peritoneal adenomucinosis [DPAM]) in a 50-year-old man with progressive abdominal distention, early satiety, and weight loss due to a ruptured low-grade appendiceal mucinous neoplasm (LAMN). **(a, b)** Axial **(a)** and coronal **(b)** T2-weighted images show heterogeneously T2-hyperintense mucin (arrowheads) surrounding the liver and stomach, with subcapsular splenic implants (∗ in **a**). Close examination of the coronal image shows marked distention of the appendix (arrow in **b**) with a "pear" or "chicken drumstick" appearance. **(c)** Photograph of the cut resected spleen shows subcapsular splenic implants (∗), which correlate with those seen at MRI. **(d)** Low-power photomicrograph of the appendix (H-E stain) shows loss of the normal mucosal architecture with proliferation of columnar mucinous epithelial cells (arrowhead), which produce mucinous content. The mucin (∗) distends the appendiceal lumen and dissects through the ruptured wall (arrows), where it implanted diffusely along the peritoneal surface, leading to PMP.

injury to the lymphatics, typically associated with surgery, such as pelvic lymphadenectomy or renal transplant.

Presenting symptoms are related to the size and location of the pseudocyst; the most common include abdominal discomfort or distention, nausea or vomiting, and an abdominal mass. CSF pseudocyst can have associated central nervous system (CNS) symptoms, such as lethargy, headache, and visual disturbances, which usually appear days or weeks after abdominal symptoms and are seldom the initial manifestation (23).

Grossly, pseudocysts have a thick wall composed of fibrous tissue, which may contain macrophages or calcifications. Pseudocysts frequently contain septa (6). There is no true epithelial lining (Fig 8, Fig E2). The collection may contain hemorrhage, pus, serous fluid, chylous fluid, CSF, or necrotic debris (6).

CT and MRI reflect this gross appearance and demonstrate a thick-walled cystic lesion, which may contain a fluid-fluid level when it contains chylous fluid (Fig 8, Fig E2) (6). Owing to the fibrous content in the wall, there will be progressive mural enhancement. Surrounding inflammatory changes are often present. At US, the pseudocyst demonstrates intracystic echogenic debris and thick walls (Fig 8, Fig E2).

CSF pseudocyst will manifest with the hallmark VP shunt tip located within the collection (Fig 7). Lymphoceles are typically found in a surgical bed, where the presence of adjacent surgical clips can narrow the differential diagnosis. Unless infected, these are typically thin walled, different from the other pseudocysts.

Peritoneal Hydatidosis.—Hydatid disease is a parasitic disease caused by *Echinococcus* and transmitted to humans via the fecal-oral route. It is commonly encountered in the liver but can be seen in the lung, spleen, kidney, heart, brain, and bones (32). Peritoneal hydatidosis comprises 10%–16% of cases of intra-abdominal hydatid disease and is often secondary to rupture of hydatid cysts in the liver or spleen. In less than 2% of patients, it can reflect primary peritoneal infection (32,33). Intraperitoneal cysts can occur anywhere in the peritoneum (32). Patients are often asymptomatic for years.

At imaging, a hydatid cyst appears as a solitary unilocular lesion or multiple well-defined cystic lesions, with or without daughter cysts (Fig 9). US is the most common imaging method used to assess hydatid disease of the abdomen. It readily demonstrates the cystic appearance and the presence of daughter cysts, floating membranes, and internal debris (6). Hydatid sand may be visible when shifting the patient's position during the examination (33). The cyst wall may contain calcification, demonstrated at plain radiography

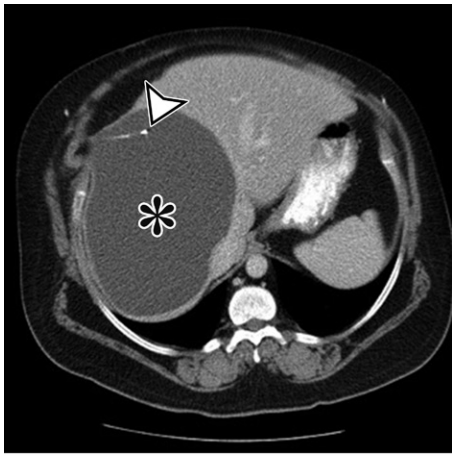

a.

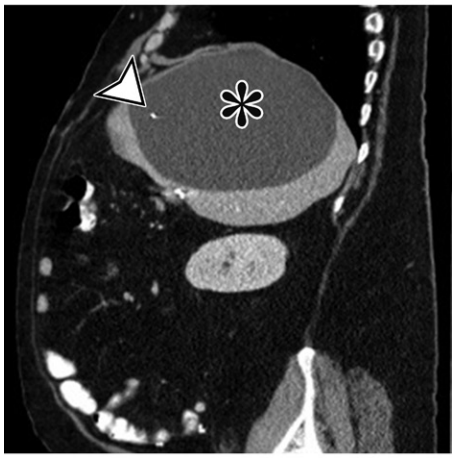

b.

Figure 7. CSF pseudocyst, also known as abdominal peritoneal pseudocyst (APC), in a 49-year-old man with a long-term ventriculoperitoneal (VP) shunt. Axial **(a)** and sagittal **(b)** contrast-enhanced CT images show a well-circumscribed thin-walled subcapsular unilocular cyst (∗) occupying nearly the entire right lobe of the liver, intimately associated with the distal tip of a VP shunt (arrowhead).

or CT (Fig 9). At MRI, the cyst wall has low T2-weighted signal intensity due to the abundant collagen content of the pericyst (Fig 9) (6).

Serologic studies are reliable in initial screening for the disease. Immunoelectrophoresis is a sensitive test for antihydatid antibodies (33), but enzyme-linked immunosorbent assay (ELISA) is more specific and can be used postoperatively to monitor the patient for recurrence (33).

Foreign Bodies.—*Textiloma* and *gossypiboma* are nonmedical terms used to describe a mass of cotton matrix unintentionally left in a body cavity during surgery. Although the real prevalence is unknown, retention of surgical sponges or swabs in the abdomen or pelvis has been reported to occur with a frequency of one in 1000–1500 for intra-abdominal operations (34).

These foreign bodies can lead to an exudative response occurring early in the postoperative course, potentially complicated by superinfection or fistula formation early or adhesions, encapsulation, and granuloma formation as a delayed response. The patient may be asymptomatic, in which case the foreign mass is found at postoperative imaging; manifests as nonspecific subacute or chronic abdominal pain; or manifests as acute infection, sepsis, or bowel obstruction. One peculiar outcome of intra-abdominal foreign bodies results from direct migration into the lumen of the bowel without fistula formation, manifesting as small-bowel obstruction at the ileocecal valve (34).

CT is the imaging study of choice for detecting gossypiboma and its potential complications (Fig 10). The typical appearance at CT is a low-attenuation heterogeneous mass with an external high-attenuation wall and a spongiform pattern containing air bubbles (Fig E3) (34). One specific but rare pattern described is a thick calcified rind (34). Most surgical sponges have a radiopaque marker, seen at CT as thin curvilinear metallic attenuation, which is pathognomonic when present (Fig 11).

There are few reports describing the MRI appearance, which can be confusing if the possibility of a foreign body is not considered (Fig E4) (34). US typically shows a well-delineated cystic or solid mass containing a wavy internal echo with a hypoechoic ring and strong posterior acoustic shadowing, caused by the retained material itself, calcified regions in the gossypiboma, or air pockets (34).

Cystic Lesions of Gastrointestinal Tract

EDC and Enteric Cyst.—EDC and enteric cyst are rare congenital anomalies found anywhere along the gastrointestinal tract from the tongue to the anus. There are two main patterns of EDC: spherical cysts (~80%), which do not communicate with the lumen, and tubular cysts (~20%), which frequently communicate with the lumen (35,36). EDC can be complicated by obstruction, intussusception, or bleeding. EDC can harbor ectopic gastric or pancreatic mucosa, leading to inflammation, bleeding, ulceration, or perforation (35,36). In adults, EDC can be incidentally identified at imaging or can be symptomatic owing to recent hemorrhage from ulceration or malignant transformation (36–38).

Pathologically, EDC arises from the mesenteric side of the bowel and is defined by an alimentary epithelial lining, an envelope of smooth muscle, and attachment to the gastrointestinal tract, sharing a wall and blood supply (35,36). Enteric cysts are similarly lined by benign enteric

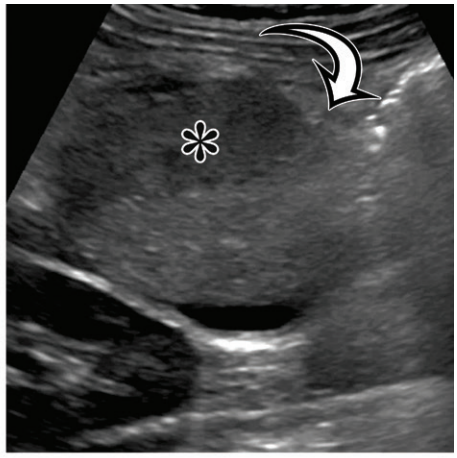

a.

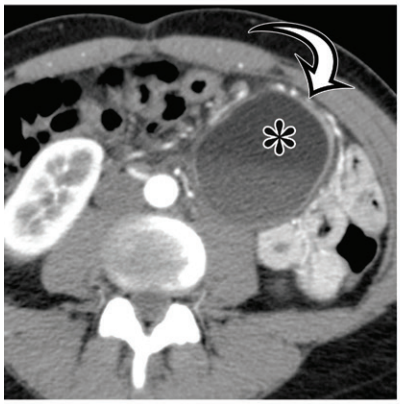

b.

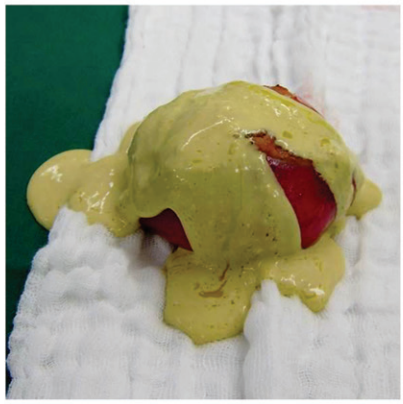

c.

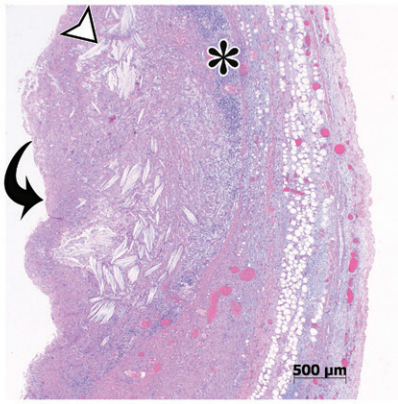

d.

Figure 8. Nonpancreatic pseudocyst in a 40-year-old woman with sudden onset of severe right upper abdominal pain, with pathologic correlation. **(a, b)** Sagittal US **(a)** and axial contrast-enhanced CT **(b)** images show a well-circumscribed complex cystic lesion centered in the left mesentery (arrow). There is a fluid-fluid level (*), with chylous fluid layering nondependently. **(c)** Photograph of the resected specimen shows thick yellow fluid oozing from the incised surface. **(d)** Low-power photomicrograph (H-E stain) shows the thick fibrous cyst wall containing cholesterol crystals (arrowhead) and lymphocytes (*), with no epithelium (arrow). Pseudocysts occur when a fibrous wall forms around fluid or a foreign body and lack a true lining.

epithelium; however, they differ from EDC in that they lack a bowel wall or organized muscle layers and are therefore considered a separate entity from EDC. Enteric cysts have only an outer disorganized muscle layer (8).

US is the preferred imaging modality for assessment of EDC. Identification of all five mural layers in a cyst (the gut signature sign) is pathognomonic of EDC and allows differentiation from enteric cysts (Fig 12) (35,39,40). Limitations of the gut signature sign include *(a)* observation in cases of torsed ovarian cyst, Meckel diverticulum, or cystic teratoma or as an artifact (39–41) and *(b)* obscuration due to the presence of inflammation or hemorrhage (35).

The split-wall sign is a newly described US finding of EDC, representing the splitting of the shared muscularis propria between the cyst and the adjacent bowel loop as a Y-shaped configuration of the hypoechoic muscular layer (35,40). Dynamic compression may enable differentiation of EDC from other abdominal cysts accurately: EDC remains attached to the bowel under compression, whereas other abdominal cysts can separate from the bowel under compression (40).

CT can delineate the location and extent of an EDC, allow assessment of complications, and assist surgical planning, but it lacks specificity (Fig E5). MRI can demonstrate the cystic nature of these lesions and their relationship to the bowel. Neither modality allows differentiation from enteric cysts, as both manifest as a unilocular thin-walled cyst when not complicated by hemorrhage, infection, or malignant degeneration. Technetium 99m pertechnetate nuclear medicine scanning can be used to detect ectopic gastric mucosa in EDC.

Mucinous Neoplasm of Appendix.—Mucinous neoplasms of the appendix are mucin-producing epithelial tumors classified into four types: adenoma, low-grade appendiceal mucinous neoplasm (LAMN), high-grade appendiceal mucinous neoplasm (HAMN), and mucinous adenocarcinoma. The peak prevalence is in middle-aged adults, with a slight female predominance (42). These tumors are typically asymptomatic and discovered incidentally at imaging, but occasionally patients present with acute appendicitis or other nonspecific abdominal symptoms related to peritoneal spread.

These neoplasms commonly appear as an appendiceal mucocele, a macroscopic description of an appendix abnormally distended with mucin

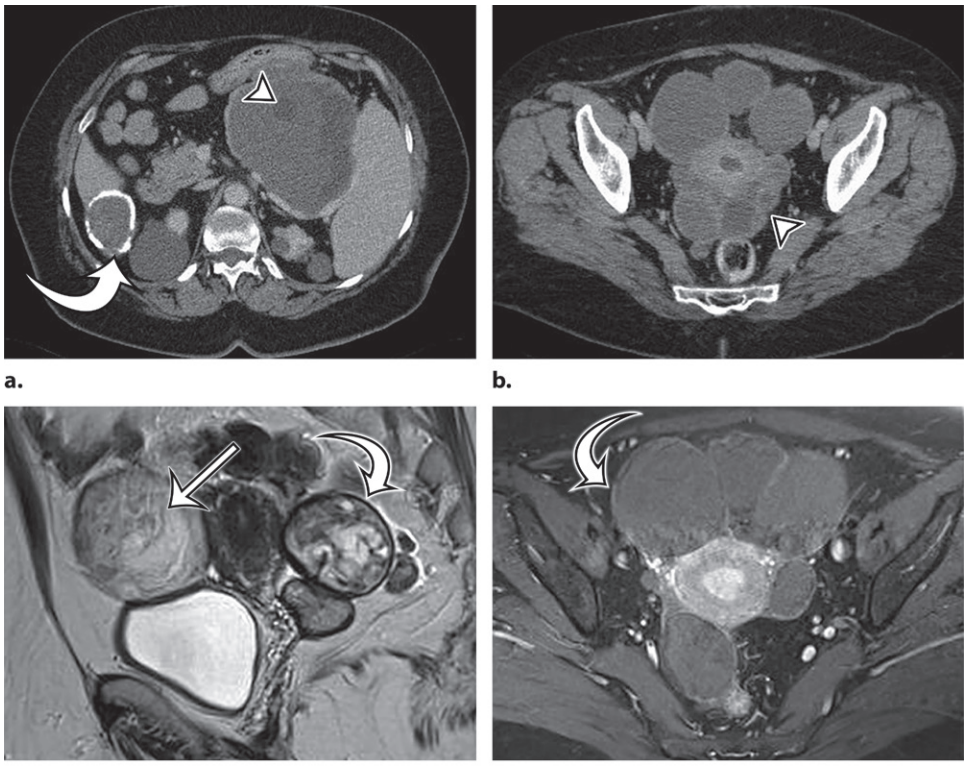

Figure 9. Peritoneal hydatidosis in an asymptomatic 49-year-old woman. **(a, b)** Axial CT images through the lower abdomen **(a)** and pelvis **(b)** show multiple well-circumscribed cystic lesions. The cyst along the posterior margin of the liver (arrow in **a**) has smooth mural calcifications. The cysts in the left upper quadrant (arrowhead in **a**) and pelvis (arrowhead in **b**) have a multiloculated appearance, with internal cysts of differing attenuation. **(c)** Sagittal T2-weighted image better shows the internal cyst architecture, including the floating inner membrane (straight arrow); the posterior pelvic cyst wall (curved arrow) is markedly T2 hypointense owing to the abundant collagen content. **(d)** Axial contrast-enhanced T1-weighted image shows enhancement of the thin walls and septa (arrow) but no internal nodularity or enhancement. Intraoperatively, there were innumerable hydatid cysts studding the peritoneum in addition to the multiple abdominal and pelvic cysts, consistent with disseminated hydatidosis, presumed secondary to a ruptured hepatic hydatid cyst.

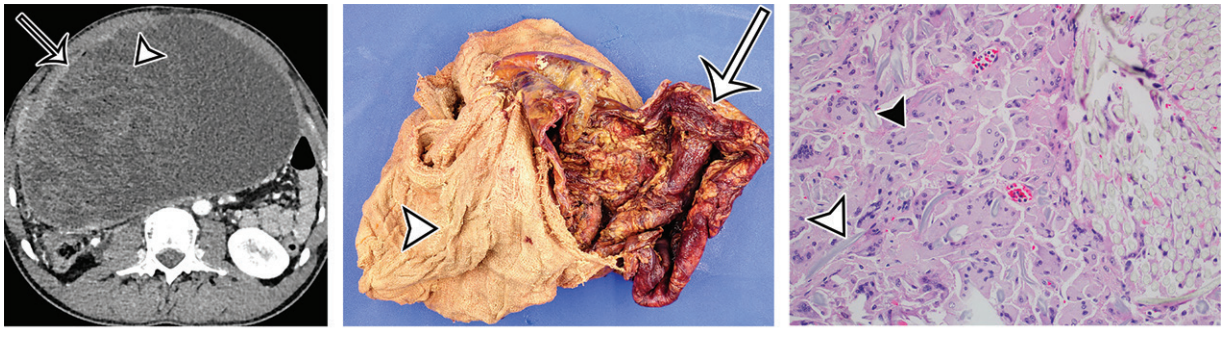

Figure 10. Foreign body in a 20-year-old man with an enlarging abdominal mass and a history of gunshot wound to the abdomen 7 years earlier. **(a)** Axial contrast-enhanced CT image shows a large complex thick-walled cystic structure (arrow) in the anterior abdomen. There are thin nonenhancing undulating internal septa (arrowhead) but no radiopaque marker. **(b)** Photograph of the gross resected specimen shows that the linear septa correlate with the folds of a surgical towel (arrowhead), encapsulated by a thick fibrous wall (arrow). **(c)** High-power photomicrograph (H-E stain) shows giant cells with invaginated (black arrowhead) and encased (white arrowhead) synthetic fibers.

(Fig 13). Appendiceal mucoceles can be caused by nonneoplastic entities or by mucin-secreting epithelial neoplasms of the appendix. Nonneoplastic entities are most commonly mucous retention cysts caused by luminal obstruction and tend to be smaller than mucinous neoplasms.

Histologically, the appendix is lined by tall columnar epithelium despite the distention (Fig

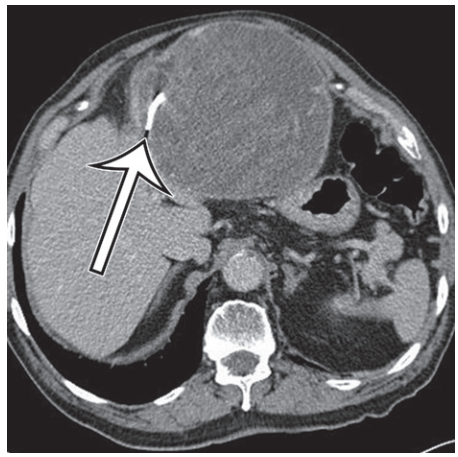

Figure 11. Foreign body in a 78-year-old man with epigastric pain. Axial contrast-enhanced CT image shows a thick-walled complex cystic structure in the epigastric anterior abdomen that contains a high-attenuation radiopaque marker (arrow), indicative of a retained surgical sponge.

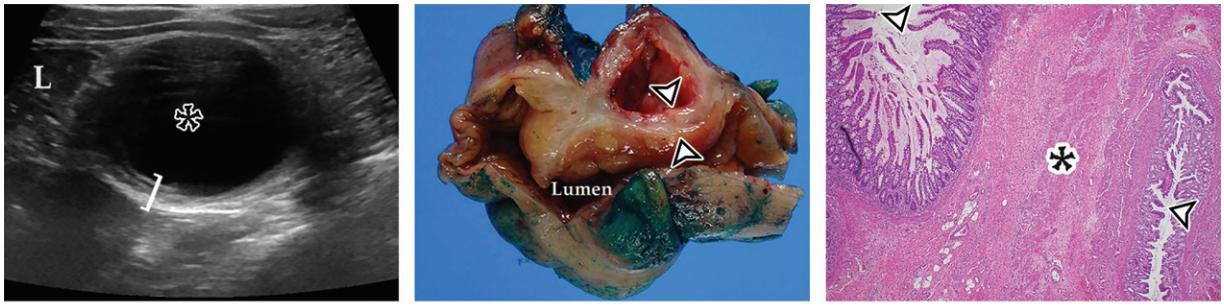

Figure 12. EDC with pathologic correlation. **(a)** Transabdominal US image at the level of the inferior margin of the liver *(L)* shows the gut signature sign (also known as the double-wall or five-layer sign) of the EDC wall. The multilayered alternating echogenic appearance resembles normal bowel, with similar innermost hyperechoic mucosa, hypoechoic muscularis mucosa, hyperechoic submucosa, hypoechoic muscularis propia, and outermost hyperechoic serosa (bracket) of the duplicated bowel wall of the EDC (∗). This cyst served as the lead point for an intussusception (shown in Fig E5) and was resected. **(b)** Photograph of a cut gross specimen shows the common wall (arrowheads) of the EDC and subjacent bowel loop. *Lumen* = small-bowel lumen. **(c)** Low-power photomicrograph (H-E stain) of an EDC shows the shared wall (∗) between the small-bowel loop and EDC. Arrowheads = mucosae.

E6), and mucin dissects through the layers of the wall; the mucin may be acellular, but there is always a focal presence of epithelial cells within the mucin. The epithelium is bland in low-grade mucinous neoplasms and dysplastic in high-grade mucinous neoplasms.

US, CT, and MRI demonstrate a markedly dilated appendix, possibly shaped like a pear or chicken drumstick (Figs 6, 13) (42), frequently with mural calcifications (Fig 13). The presence of an appendiceal mucocele should prompt a search for extraluminal mucin: low-attenuation deposits limited to the periappendiceal region or disseminated throughout the peritoneal cavity (Fig 6) (42).

Differential Diagnosis

The anatomic location and imaging features of a cystic lesion encountered in the abdomen are the most important factors to consider when establishing a radiologic differential diagnosis. The lesions highlighted in this article arise from the mesentery, peritoneum, or gastrointestinal tract. However, these and other cystic lesions may arise from solid abdominal organs (liver, spleen, pancreas) or from pelvic organs (urachus, adnexal organs) as well.

Hepatic- and splenic-origin cystic lesions can be classified as developmental, inflammatory, neoplastic, or trauma-related; the most common are simple liver cysts and biliary hamartomas, usually encountered incidentally at imaging (Fig E7) (43,44). Pancreatic cystic lesions including pancreatic pseudocyst, MCN, intraductal papillary mucinous neoplasm (IPMN), serous cystadenoma, and solid-pseudopapillary neoplasm (SPN) have well-described imaging features (Figs 14, 15; Figs E8, E9) (45). Cystic degeneration or necrosis within a ductal adenocarcinoma, neuroendocrine tumor, or acinar cell carcinoma may also have a cystic appearance.

In the pelvis, cystic lesions can arise from the urachal remnant or reproductive organs. Residual patency of some or all of the urachus can lead to a cystic-appearing lesion in the anterior pelvis, characteristically between the anterosuperior bladder dome and umbilicus (Fig 16, Fig E10) (46). Cystic lesions arising from the ovaries are com-

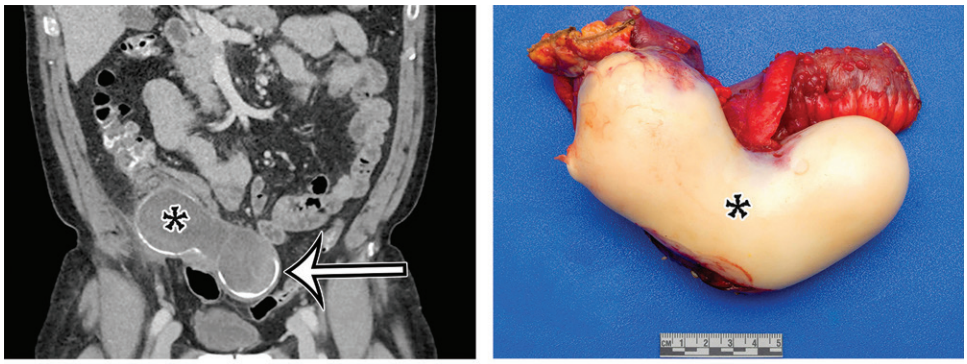

a. b.

Figure 13. Appendiceal mucinous neoplasm in a 64-year-old man with right lower quadrant pain. **(a)** Coronal contrast-enhanced CT image shows marked distention of the appendix, with heterogeneous internal contents (*) and curvilinear calcification of the appendiceal wall (arrow). **(b)** Photograph of the intact resected specimen shows a mucin-distended rubbery appendix (*). Histopathologic analysis of the appendiceal wall demonstrated tall columnar mucinous bland epithelium, seen with low-grade appendiceal mucinous neoplasms (LAMNs) (Fig E6).

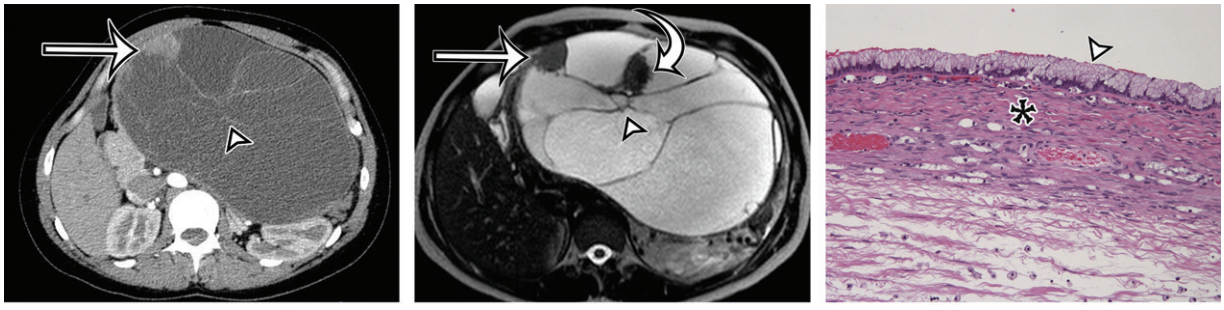

a. b. c.

Figure 14. Pancreatic MCN in a 28-year-old woman with early satiety and increasing abdominal girth. **(a)** Axial contrast-enhanced CT image shows a large multiloculated thin-walled cystic mass in the anterior left upper quadrant with thin septa (arrowhead) and a solid nodular component (arrow). **(b)** Axial T2-weighted image shows a similar imaging appearance, with improved conspicuity of an additional solid nodule (curved arrow). Straight arrow = solid nodular component in **a**, arrowhead = septa. **(c)** Histologic image of the cyst wall shows columnar mucin-producing epithelium (arrowhead) with underlying ovarian stroma (*), a diagnostic feature of MCN. (H-E stain; original magnification, ×100.)

mon and are frequently encountered incidentally at imaging performed for evaluation of pelvic and abdominal complaints; determining adnexal origin can be difficult for large lesions (Fig 17).

When the cystic lesion is large, determining the site of origin may be difficult, forcing reliance on imaging features to establish the differential diagnosis. Locularity and the presence of solid nodules are the most useful features, serving as a basis for an algorithmic approach to making the diagnosis or establishing a useful differential diagnosis (Table 2; Figs E11, E12).

Unilocular cysts without solid nodules are nonneoplastic (Fig E11). Mesenteric true cysts are thin walled without septa; EDCs and enteric cysts are thin walled with septa. Nonpancreatic pseudocyst and gossypiboma are unilocular with a thick fibrous wall.

Mucinous neoplasms should be considered for a unilocular cyst with solid components, which may arise from the appendix (low-grade appendiceal mucinous neoplasm [LAMN]) or mesentery, pancreas, ovary, or liver (MCN).

Multilocularity can be present in neoplastic (benign or malignant), infectious, inflammatory, or congenital lesions (Fig E12). Thin-walled multilocular cystic lesions without solid nodules are almost always benign, with the exception of pseudomyxoma peritonei or mucinous carcinomatosis, which should be considered when a mucinous neoplasm is present (LAMN, MCN, gastrointestinal tract mucinous adenocarcinoma). LAMN can appear as or contain solid components. Demographics and location can help distinguish lymphangioma, MCPM, pancreatic solid-pseudopapillary neoplasm (SPN), and pancreatic or ovarian serous cystadenoma. Correlation with clinical features can help distinguish peritoneal hydatidosis from MCN or pseudocyst.

The presence of solid nodular components in a multilocular cyst should raise concern for malignant or malignant-potential neoplasm.

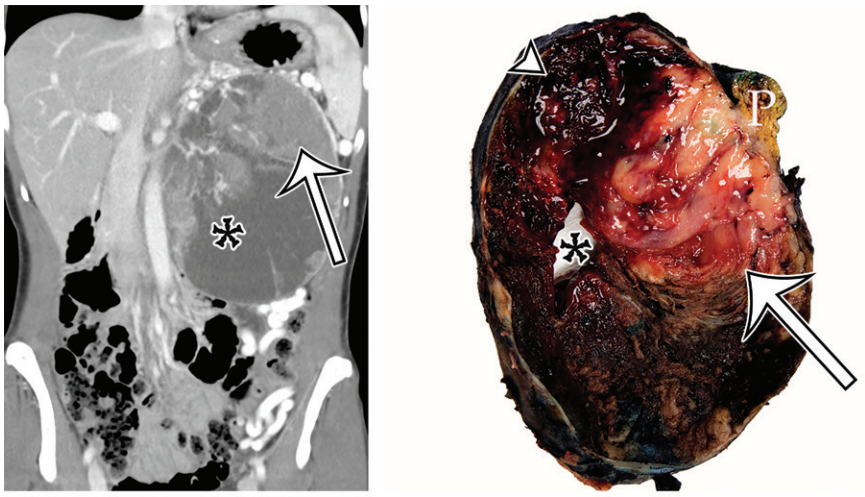

Figure 15. Pancreatic solid-pseudopapillary neoplasm (SPN) in a 42-year-old woman. **(a)** Coronal contrast-enhanced CT image shows a large solid (arrow) and cystic (*) tumor centered in the left upper quadrant, but of unclear origin. **(b)** Photograph of the cut resected specimen shows that the tumor arises from the pancreas *(P)*. The tan-pink viable tissue (arrow) corresponds to the area of solid components seen at CT, and the hemorrhagic (arrowhead) and cystic necrotic (*) components correspond to similar areas seen at CT.

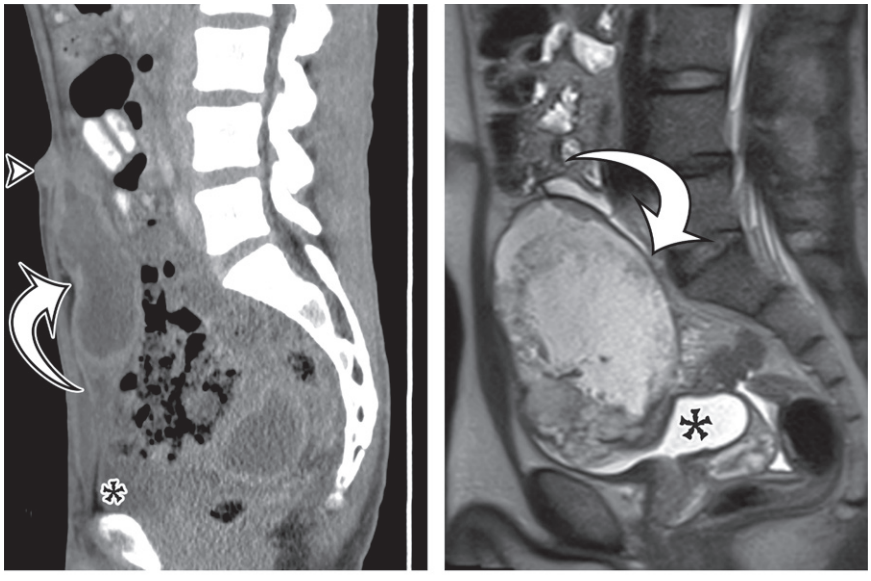

Figure 16. Spectrum of urachus-origin cystic lesions. **(a)** Urachal sinus in a 44-year-old man with sanguineous fluid draining from the umbilicus. Sagittal CT image shows a fluid-filled tubular structure (arrow) just deep to the anterior abdominal wall, extending from the umbilicus (arrowhead) to the bladder dome (*). **(b)** Urachal adenocarcinoma arising in a urachal diverticulum in a 57-year-old man. Sagittal T2-weighted image shows a large heterogeneous cystic mass (arrow) just deep to the anterior abdominal wall, which exerts mass effect on the bladder dome (*). (See Fig E10 for additional images.)

Specifically, thick-walled cystic lesions with solid components should raise concern for MCN (mesentery, pancreas, liver, or ovary) or ovarian cystic neoplasm (cystadenocarcinoma or teratoma).

Finally, knowledge of clinically important mimics can reduce the risk of misinterpretation and delayed management. Solid soft-tissue neoplasms (sarcoma, GISTs, desmoid tumors), mesenteric metastases (from the colon or pancreas), and mesenteric lymph nodes (*Mycobacterium avium-intracellulare* [MAI] infection, tuberculosis) can have a substantial cystic component—usually due to cystic, hemorrhagic, or necrotic degeneration—or a myxoid component (47–49). Larger GISTs can demonstrate central areas of low attenuation, corresponding to hemorrhage, necrosis, or cyst formation (Fig 18) (50). Intratumoral cystic changes are associated with increasing size and are frequently seen in high-risk GISTs (Fig 18) (51).

Myxoid components of soft-tissue non-GIST sarcomas and desmoid tumors are hypoattenuating at CT with high T2-weighted signal intensity at MRI (Fig 19) and can mimic the appearance of a cystic lesion. Enhancement of the myxoid matrix distinguishes it from a cystic mass; this is best observed at MRI, aided by use of subtraction postprocessing. Thick enhancing septa characteristically course through the mass and correspond to fibrous bands coursing through the myxoid stroma. Desmoid tumor cannot be differentiated from sarcoma with myxoid elements, and biopsy is necessary to establish the diagnosis.

Management

Surgical resection is the treatment of choice for most cystic lesions in the abdomen. True cystic

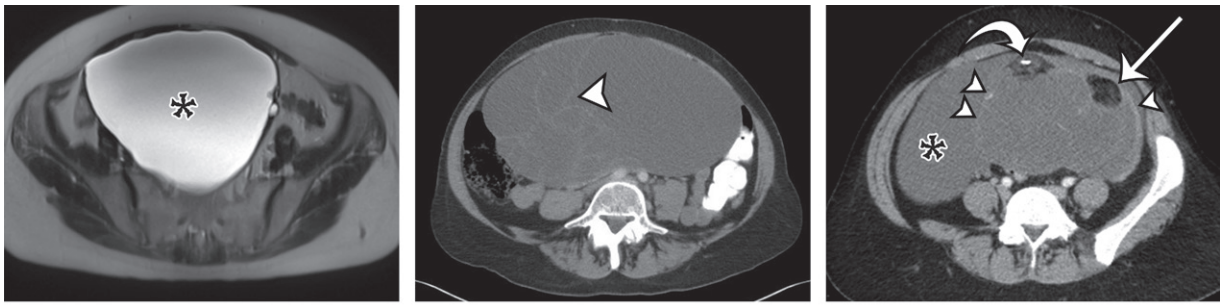

a. b. c.

Figure 17. Spectrum of adnexal-origin cystic masses. **(a)** Axial T2-weighted image in a 67-year-old woman with right lower quadrant pain shows homogeneous hyperintense signal in a well-circumscribed unilocular thin-walled cyst (*), which was found to arise from the right ovary. Histologic analysis showed benign epithelium, consistent with serous cystadenoma. **(b)** Axial contrast-enhanced image in a 62-year-old woman with increasing abdominal girth shows a well-circumscribed multiloculated cyst with multiple thin septa (arrowhead) but no mural nodules. Surgically, the cyst was found to arise from the right ovary. Histologic analysis showed a single layer of mucinous epithelium, consistent with MCN. **(c)** Axial contrast-enhanced CT image in a 32-year-old woman with increasing abdominal pain shows a large multiloculated cystic mass (arrowheads) in the midline pelvis, which contains calcification (curved arrow) and fat (straight arrow) and is surrounded by ascites (*). The mass was found to arise from the left ovary. Histologically, it was shown to be a mature cystic teratoma.

Table 2: Imaging Characteristics of Cystic Lesions Found in and around the Peritoneal Cavity

Type of Cystic Lesion	Content	Locularity*	Wall Thickness	Septa	Solid Nodule	Calcifications
Simple peritoneal cyst	Simple (serous)	Unilocular	Thin	No	No	No
Chylolymphatic mesenteric cyst	Simple (serous) Chylous (fat-fluid level)	Unilocular	Thin	No	No	No
Cystic lymphangioma	Simple (serous)	Multilocular Unilocular (rare)	Thin	Yes	No	Rare
Mucinous cystic neoplasm of mesentery	Complex (mucin, blood)	Multilocular >> unilocular	Thin or thick	Yes	Rare (worrisome feature)	Mural and septal
Multicystic peritoneal mesothelioma	Simple (serous) Debris or blood rare	Multilocular >> unilocular	Thin	Yes	Possible	No
Pseudomyxoma peritonei	Complex (mucinous)	Multilocular >> unilocular	Thin	No	No	Curvilinear mural
Nonpancreatic pseudocyst	Complex (blood, pus, fat, fluid)	Unilocular > multilocular	Thick	Yes	No	Mural
Peritoneal hydatidosis	Daughter cysts Condensed maternal fluid	Multilocular, unilocular	Thin or thick	Floating membranes	No	Mural
Peritoneal tuberculosis	Complex (proteinaceous)	Loculated ascites	Thick	No	No	Present
Foreign bodies	Complex	Unilocular	Thick	Undulating fibers, spongiform	No	Mural

*> = more common than, >> = much more common than.

lesions—including peritoneal simple mesothelial cyst (PSMC), symptomatic chylolymphatic cysts, small cystic lymphangiomas, and enteric cysts (EDC and enteric cyst)—are benign and have a highly favorable prognosis. Total excision is curative with minimal risk of complications and no risk of recurrence (2,7,10,12,13). Of note, complete resection of larger more infiltrative cystic lymphangiomas is difficult; thus, recurrence is more likely (12).

Pseudocysts are less often excised, with medical therapy, drainage, and marsupialization more

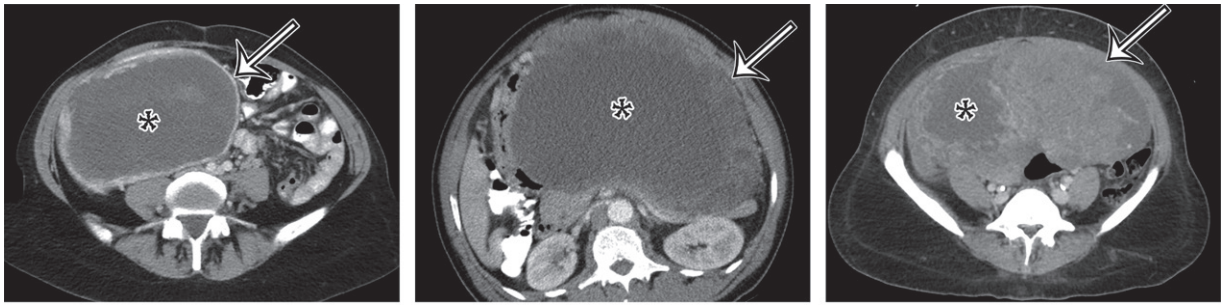

a. b. c.

Figure 18. Spectrum of cystic gastrointestinal stromal tumor (GIST) at axial contrast-enhanced CT. **(a)** Axial contrast-enhanced CT image in a 35-year-old woman with right-sided bulging of the abdomen shows a large unilocular thick-walled cyst in the right abdomen (arrow) with no obvious site of origin. The internal contents have heterogeneous attenuation (*). **(b)** Axial contrast-enhanced CT image in a 61-year-old man with new-onset abdominal pain similarly shows a large predominantly unilocular cystic mass (*) in the anterior abdomen, with a thick wall (arrow) and mass effect on the pancreas and stomach but no clear site of origin. **(c)** Axial contrast-enhanced CT image in a 50-year-old woman shows a solid and cystic mass in the anterior abdomen. The cystic components (*) are more loculated, with thick walls and large solid components (arrow), consistent with cystic degeneration of a high-risk GIST.

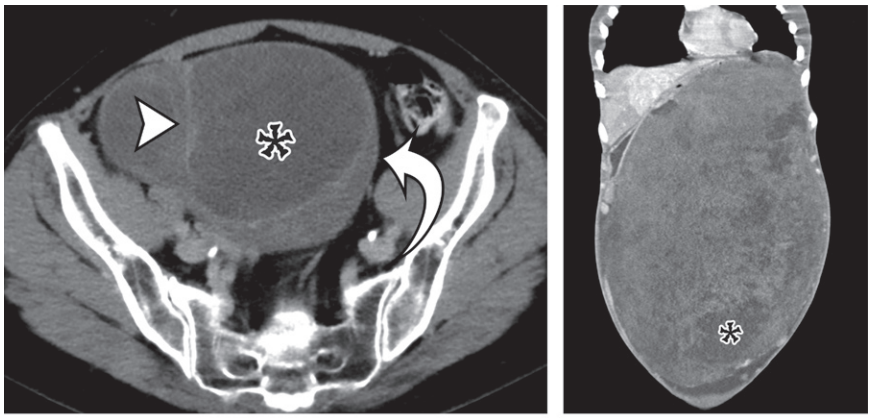

a. b.

Figure 19. Spectrum of cystic-appearing soft-tissue tumors. **(a)** Axial contrast-enhanced CT image in a 62-year-old woman with a palpable abdominal mass shows a large thick-walled multiloculated cystic mass (*) with septa (arrowhead) and solid nodular components (arrow). It was pathologically confirmed to be dedifferentiated liposarcoma with myxoid components, which corresponded to the cystic spaces. **(b)** Coronal contrast-enhanced CT image in an 18-year-old woman with abdominal distention and pain shows a massive predominantly solid mass with several cystic components (*). At histopathologic evaluation, the cystic components corresponded to areas of myxoid stroma within a spindle cell tumor, consistent with desmoid tumor. Desmoid tumors have invasive properties and tend to damage blood vessels.

commonly used (52,53). CSF pseudocysts are typically managed by removal of the catheter and administration of antibiotics until results of the final cultures are negative or the superimposed infection is resolved (23).

Similarly, peritoneal infections are managed medically and surgically. Peritoneal hydatidosis is managed medically with albendazole or praziquantel, with or without surgical excision. When surgical excision is performed, complete excision with no spillage is the goal (33). Puncture, aspiration, injection, and reaspiration (PAIR) is also a proven successful treatment (33). Rupture and dissemination are known complications of hydatid disease; one potential complication of rupture is anaphylaxis (33).

Management of localized neoplasms is primarily surgical. MCNs are resected owing to the risk of malignant transformation (14,15). As appendiceal mucinous neoplasms may manifest with obstructive appendicitis or superinfection that is otherwise clinically indistinguishable from typical appendicitis, recognizing the possibility of appendiceal neoplasm preoperatively has significant surgical implications (appendectomy vs right hemicolectomy) (54). Appendiceal diameter greater than 1.5 cm and morphologic changes (soft-tissue mass or cystic dilatation) should raise suspicion of neoplasm of the appendix (54).

More infiltrative and diffuse peritoneal disease, including MCPM and PMP, is difficult to treat surgically. MCPM has a 50% recurrence rate

after resection, typically within the first few years, with some reports of recurrence up to 27 years after surgery (17,18). Owing to the high recurrence rate and the potential for malignant transformation, some studies propose an aggressive approach using cytoreductive surgery with extended peritonectomy associated with hyperthermic intraperitoneal chemotherapy (CRS-HIPEC) (17). PMP is similarly treated with aggressive surgical debulking and CRS-HIPEC (20).

Selecting optimal candidates for CRS-HIPEC is important to increase the likelihood of complete cytoreduction and achieve long-term survival benefits for a procedure that otherwise carries high risk of morbidity. Various quantitative prognostic scoring systems have been developed for that purpose. The most widely used is the peritoneal cancer index (PCI) developed by Jacquet and Sugarbaker (55), which assesses tumor volume and distribution intraoperatively (56).

Preoperative imaging assessment can be valuable to the surgeon in determining preoperative score and estimating therapeutic prognosis (56,57). Therefore, the radiology report should detail the spread of the disease, describing the primary tumor whenever possible and detailing the organs involved. Certain peritoneal locations portend worse prognosis and predict incomplete cytoreduction and therefore warrant explicit comment in the report: porta hepatis (infiltration with or without bile duct obstruction), mesentery (infiltration or mesenteric foreshortening, also known as cocoon abdomen or frozen abdomen), small bowel (obstruction or jejunal involvement with a mass >5 cm), and gastrohepatic or hepatoduodenal ligament (subpyloric space tumor, gastrohepatic ligament disease >5 cm).

Additional extraperitoneal disease should be explicitly mentioned: retroperitoneum (hydroureter, psoas invasion, and retroperitoneal lymphadenopathy) and abdominal wall or pelvic sidewall invasion. The presence of serous or hemorrhagic ascites is also a poor prognostic sign. Finally, parenchymal metastasis to the liver, pancreas, or spleen should be clearly mentioned, particularly since they cannot be assessed laparoscopically.

Patients with PMP arising from an appendiceal low-grade mucinous neoplasm have a 5-year survival rate exceeding 50% (19,20), far better than that of mucinous carcinomatosis, which bestows a 5-year survival rate of less than 10% (19).

Conclusion

Cystic-appearing lesions in the abdomen and pelvis can have a broad differential diagnosis encompassing neoplastic, inflammatory, congenital, and iatrogenic lesions. While some lesions are truly cystic, others may represent necrosis, cystic degeneration, hematomas, or reactive collections. The distinction may not always be evident at imaging; however, careful assessment of the imaging appearance (Table 2; Figs E11, E12), location, relationship to surrounding structures, and clinical context may help narrow the differential diagnosis and guide management.

Acknowledgment.—We would like to thank Marion L. Hartley, PhD, for her careful edits and suggestions during composition of the manuscript.

Disclosures of Conflicts of Interest.—**M.A.M.** *Activities related to the present article:* Editorial board member of *RadioGraphics* (not involved in the handling of this article). *Activities not related to the present article:* disclosed no relevant relationships. *Other activities:* disclosed no relevant relationships.

References

1. de Perrot M, Bründler M, Tötsch M, Mentha G, Morel P. Mesenteric cysts: toward less confusion? Dig Surg 2000;17(4):323–328.
2. Ousadden A, Elbouhaddouti H, Ibnmajdoub KH, Harmouch T, Mazaz K, Aittaleb K. A giant peritoneal simple mesothelial cyst: a case report. J Med Case Reports 2011;5(1):361.
3. Comoglio C, Sansone F, Delsedime L, Campanella A, Ceresa F, Rinaldi M. Mesothelial cyst of the pericardium, absent on earlier computed tomography. Tex Heart Inst J 2010;37(3):354–357.
4. Carboni F, Valle M, Camperchioli I, Levi Sandri GB, Sentinelli S, Garofalo A. Mesothelial cyst of the round ligament of the liver. J Minim Access Surg 2016;12(1):83–85.
5. Lee S, Kwon J, Kim Y, Kim K. Peritoneal Simple Mesothelial Cyst Misdiagnosed as a Gastric Subepithelial Tumor. J Gastrointest Surg 2017;21(9):1555–1556.
6. Arraiza M, Metser U, Vajpeyi R, et al. Primary cystic peritoneal masses and mimickers: spectrum of diseases with pathologic correlation. Abdom Imaging 2015;40(4):875–906.
7. Lee DLP, Madhuvrata P, Reed MW, Balasubramanian SP. Chylous mesenteric cyst: a diagnostic dilemma. Asian J Surg 2016;39(3):182–186.
8. Rattan KN, Nair VJ, Pathak M, Kumar S. Pediatric chylolymphatic mesenteric cyst: a separate entity from cystic lymphangioma—a case series. J Med Case Reports 2009;3(1):111.
9. Wang J, Fisher C, Thway K. Combined mesothelial cyst and lymphangioma of the small bowel: a distinct hybrid intra-abdominal cyst. Int J Surg Pathol 2014;22(6):547–551.
10. de la Plaza Llamas R, Ramia Ángel JM, García Amador C, López Marcano AJ. Chylous Mesenteric Cyst. J Gastrointest Surg 2018;22(5):921–922.
11. Chan WYS, Kwan KEL, Teo LT. A rare case of retroperitoneal and mesenteric lymphangiomatosis. Radiol Case Rep 2019;15(1):11–14.
12. Wani I. Mesenteric lymphangioma in adult: a case series with a review of the literature. Dig Dis Sci 2009;54(12):2758–2762.
13. Hornick JL, Fletcher CDM. Intraabdominal cystic lymphangiomas obscured by marked superimposed reactive changes: clinicopathological analysis of a series. Hum Pathol 2005;36(4):426–432.
14. Metaxas G, Tangalos A, Pappa P, Papageorgiou I. Mucinous cystic neoplasms of the mesentery: a case report and review of the literature. World J Surg Oncol 2009;7(1):47.
15. Cauchy F, Lefevre JH, Mourra N, Parc Y, Tiret E, Balladur P. Mucinous cystadenoma of the mesocolon, a rare entity frequently presenting with features of malignity: two case reports and review of the literature. Clin Res Hepatol Gastroenterol 2012;36(1):e12–e16.
16. WHO Classification of Tumours Editorial Board. Digestive System Tumours. In: WHO Classification of Tumours.

5th ed. Lyon, France: International Agency for Research on Cancer, 2019.
17. Noiret B, Renaud F, Piessen G, Eveno C. Multicystic peritoneal mesothelioma: a systematic review of the literature. Pleura Peritoneum 2019;4(3):20190024.
18. Levy AD, Arnáiz J, Shaw JC, Sobin LH. Primary peritoneal tumors: imaging features with pathologic correlation. RadioGraphics 2008;28(2):583–607; quiz 621–622.
19. Levy AD, Shaw JC, Sobin LH. Secondary tumors and tumorlike lesions of the peritoneal cavity: imaging features with pathologic correlation. RadioGraphics 2009;29(2):347–373.
20. García KM, Flores KM, Ruiz A, González FL, Rodríguez ÁM. Pseudomyxoma Peritonei: Case Report and Literature Review. J Gastrointest Cancer 2019;50(4):1037–1042.
21. Carr NJ, Cecil TD, Mohamed F, et al. A Consensus for Classification and Pathologic Reporting of Pseudomyxoma Peritonei and Associated Appendiceal Neoplasia: The Results of the Peritoneal Surface Oncology Group International (PSOGI) Modified Delphi Process. Am J Surg Pathol 2016;40(1):14–26.
22. Diop AD, Fontarensky M, Montoriol PF, Da Ines D. CT imaging of peritoneal carcinomatosis and its mimics. Diagn Interv Imaging 2014;95(9):861–872.
23. Anderson CM, Sorrells DL, Kerby JD. Intraabdominal pseudocysts as a complication of ventriculoperitoneal shunts. J Am Coll Surg 2003;196(2):297–300.
24. Tamura A, Shida D, Tsutsumi K. Abdominal cerebrospinal fluid pseudocyst occurring 21 years after ventriculoperitoneal shunt placement: a case report. BMC Surg 2013;13(1):27.
25. Kaplan M, Ozel SK, Akgun B, Kazez A, Kaplan S. Hepatic pseudocyst as a result of ventriculoperitoneal shunts: case report and review of the literature. Pediatr Neurosurg 2007;43(6):501–503.
26. Banka S, Johnson K, Sgouros S. Liver cyst caused by the peritoneal catheter of a CSF shunt. Pediatr Neurosurg 2007;43(5):444–445.
27. Arsanious D, Sribnick E. Intrahepatic Cerebrospinal Fluid Pseudocyst: A Case Report and Systematic Review. World Neurosurg 2019;125:111–116.
28. Dabdoub CB, Fontoura EA, Santos EA, Romero PC, Diniz CA. Hepatic cerebrospinal fluid pseudocyst: a rare complication of ventriculoperitoneal shunt. Surg Neurol Int 2013;4(1):162.
29. Faraj W, Ahmad HH, Mukherji D, Khalife M. Hepatic cerebrospinal fluid pseudocyst mimicking hydatid liver disease: a case report. J Med Case Reports 2011;5(1):475.
30. Bettis T, Holsten S, Mitchell A. Conservative Management of a Hepatic CSF Pseudocyst in an Asymptomatic Patient. Am Surg 2019;85(8):e389–e391.
31. Guest BJ, Merjanian MH, Chiu EF, Canders CP. Abdominal Cerebrospinal Fluid Pseudocyst Diagnosed with Point-of-Care Ultrasound. Clin Pract Cases Emerg Med 2019;3(1):43–46.
32. Lianos GD, Lazaros A, Vlachos K, et al. Unusual locations of hydatid disease: a 33 year's experience analysis on 233 patients. Updates Surg 2015;67(3):279–282.
33. Hegde N, Hiremath B. Primary peritoneal hydatidosis. BMJ Case Rep 2013;2013:bcr2013200435.
34. Manzella A, Filho PB, Albuquerque E, Farias F, Kaercher J. Imaging of gossypibomas: pictorial review. AJR Am J Roentgenol 2009;193(6 suppl):S94–S101.
35. Sangüesa Nebot C, Llorens Salvador R, Carazo Palacios E, Picó Aliaga S, Ibañez Pradas V. Enteric duplication cysts in children: varied presentations, varied imaging findings. Insights Imaging 2018;9(6):1097–1106.
36. Macpherson RI. Gastrointestinal tract duplications: clinical, pathologic, etiologic, and radiologic considerations. RadioGraphics 1993;13(5):1063–1080.
37. Gümüş M, Kapan M, Gümüş H, Önder A, Girgin S. Unusual noncommunicating isolated enteric duplication cyst in adults. Gastroenterol Res Pract 2011;2011:323919.
38. Kim SK, Lim HK, Lee SJ, Park CK. Completely isolated enteric duplication cyst: case report. Abdom Imaging 2003;28(1):12–14.
39. Fonseca EKUN, Sameshima YT. Gut signature sign in enteric duplication cysts. Abdom Radiol (NY) 2018;43(12):3513–3514.
40. Kitami M. Dynamic Compression: A New and Practical Technique for the Sonographic Diagnosis of Enteric Duplication. Ultrasound Q 2019;35(4):385–391.
41. Cheng G, Soboleski D, Daneman A, Poenaru D, Hurlbut D. Sonographic pitfalls in the diagnosis of enteric duplication cysts. AJR Am J Roentgenol 2005;184(2):521–525.
42. Leonards LM, Pahwa A, Patel MK, Petersen J, Nguyen MJ, Jude CM. Neoplasms of the Appendix: Pictorial Review with Clinical and Pathologic Correlation. RadioGraphics 2017;37(4):1059–1083.
43. Borhani AA, Wiant A, Heller MT. Cystic hepatic lesions: a review and an algorithmic approach. AJR Am J Roentgenol 2014;203(6):1192–1204. [Published correction appears in AJR Am J Roentgenol 2015;204(2):459.]
44. Urrutia M, Mergo PJ, Ros LH, Torres GM, Ros PR. Cystic masses of the spleen: radiologic-pathologic correlation. RadioGraphics 1996;16(1):107–129.
45. Foster BR, Jensen KK, Bakis G, Shaaban AM, Coakley FV. Revised Atlanta Classification for Acute Pancreatitis: A Pictorial Essay. RadioGraphics 2016;36(3):675–687.
46. Parada Villavicencio C, Adam SZ, Nikolaidis P, Yaghmai V, Miller FH. Imaging of the Urachus: Anomalies, Complications, and Mimics. RadioGraphics 2016;36(7):2049–2063.
47. Levy AD, Manning MA, Miettinen MM. Soft-Tissue Sarcomas of the Abdomen and Pelvis: Radiologic-Pathologic Features. II. Uncommon Sarcomas. RadioGraphics 2017;37(3):797–812.
48. Levy AD, Manning MA, Al-Refaie WB, Miettinen MM. Soft-Tissue Sarcomas of the Abdomen and Pelvis: Radiologic-Pathologic Features. I. Common Sarcomas. RadioGraphics 2017;37(2):462–483.
49. Turgeon MK, Cardona K. Soft Tissue Tumors of the Abdomen and Retroperitoneum. Surg Clin North Am 2020;100(3):649–667.
50. Levy AD, Remotti HE, Thompson WM, Sobin LH, Miettinen M. Gastrointestinal stromal tumors: radiologic features with pathologic correlation. RadioGraphics 2003;23(2):283–304, 456; quiz 532.
51. Yu MH, Lee JM, Baek JH, Han JK, Choi BI. MRI features of gastrointestinal stromal tumors. AJR Am J Roentgenol 2014;203(5):980–991.
52. Oxenberg J. Giant Intraperitoneal Multiloculated Pseudocyst in a Male. Case Rep Surg 2016;2016:4974509.
53. Oray-Schrom P, St Martin D, Bartelloni P, Amoateng-Adjepong Y. Giant nonpancreatic pseudocyst causing acute anuria. J Clin Gastroenterol 2002;34(2):160–163.
54. Pickhardt PJ, Levy AD, Rohrmann CA Jr, Kende AI. Primary neoplasms of the appendix manifesting as acute appendicitis: CT findings with pathologic comparison. Radiology 2002;224(3):775–781.
55. Jacquet P, Sugarbaker PH. Clinical research methodologies in diagnosis and staging of patients with peritoneal carcinomatosis. Cancer Treat Res 1996;82:359–374.
56. Bartlett DJ, Thacker PG Jr, Grotz TE, et al. Mucinous appendiceal neoplasms: classification, imaging, and HIPEC. Abdom Radiol (NY) 2019;44(5):1686–1702.
57. Sugarbaker PH, Sardi A, Brown G, Dromain C, Rousset P, Jelinek JS. Concerning CT features used to select patients for treatment of peritoneal metastases: a pictoral essay. Int J Hyperthermia 2017;33(5):497–504.